Segmentation of building roofs from airborne LiDAR point clouds using robust voxel-based region growing

Yusheng Xu, Wei Yao, Ludwig Hoegner & Uwe Stilla

Published online: 16 Jul 2017.

Submit your article to this journal ☐

Article views: 206

View Crossmark data ☐

Citing articles: 3 View citing articles ☐

Taylor & Francis
Taylor & Francis Group

Check for updates

Segmentation of building roofs from airborne LiDAR point clouds using robust voxel-based region growing

Yusheng Xu [iD][a], Wei Yao[a,b], Ludwig Hoegner[a] and Uwe Stilla[a]

[a]Photogrammetry and Remote Sensing, Technische Universität München, Munich, Germany; [b]Department of Geoinformation, Munich University of Applied Sciences, Munich, Germany

ABSTRACT

The research herein presents a new approach for extracting building roofs using a robust voxel-based region growing segmentation method. The proposed approach exploits the fact that the roof of the building consists of planar surfaces and has distinctive geometric features than other kinds of objects. Based on this assumption, we present a method using voxel structure and region growing strategy with robust principal component analysis (RPCA). The voxels is clustered by a region growing process, utilizing the smoothness, continuity, and convexity as geometric cues. RPCA is introduced to estimate the attribute of voxels. Roofs are recognized from the segments by using the object-based spectral clustering. Our approach has been validated by different airborne laser scanning (ALS) point clouds. Qualitative and quantitative results reveal that our method outperforms some representative algorithms in segmentation using our testing datasets under a complex situation, with overall quality measure better than 0.7 and 0.6.

1. Introduction

In recent years, laser scanning technology has become the most efficient surveying technique for acquiring detailed and accurate measurements for three-dimensional (3D) building reconstruction. By using light detection and ranging (LiDAR) technique, large volumes of highly accurate and densely sampled measuring points are obtained, largely enriching the data source for 3D building reconstruction and greatly simplifying the data acquisition procedure, because the scanned laser point has direct 3D coordinates and the representation of scenes (Vo et al. 2016). However, due to the large amount of datasets, complex structures of scenes, outliers, and highly variable points densities, to recognize and extract objects from point clouds is still a challenging task. To this end, segmentation algorithms are normally adopted to partition the unstructured raw point cloud into meaningful segments with geometric consistency.

Segmentation plays a vital role in the 3D building model reconstruction (Truong-Hong et al. 2013). However, conventional algorithms is always restrained by complex scenes and the data

---

quality. Specifically, the point density will vary with the incidence angle of laser beam and observation distances. The point density of facades and roofs in the same building can be significantly different. For point-based segmentation methods like region growing and its variants (Rabbani, Van Den Heuvel, and Vosselmann 2006) or classification-based method (Weinmann et al. 2015; Wang et al. 2015), normally defining a 3D neighborhood (Truong-Hong et al. 2013) (e.g., points in a 3D sphere or k-nearest neighbors) to estimate the geometric information (e.g., normals or features) of individual point. However, the varying point density requires a flexible or adaptive size of 3D neighborhood, for collecting enough points in low density areas. Besides, compared with model-based segmentation methods (Schnabel, Wahl, and Klein 2007; Chen et al. 2012), the region growing methods are more sensitive to noise and outliers in the datasets. For example, moving vehicles and pedestrians may result in outliers in measured ALS dataset, causing failure in the growing. To overcome these drawbacks, higher level elements (e.g., 3D patches or slices) are introduced. For instance, voxel-based methods (Truong-Hong et al. 2013; Aljumaily, Laefer, and Cuadra 2015) are the representatives, in which the bounding box of the entire point cloud is partitioned with 3D grid and points inside the cubic is defined as a voxel. With the voxel representation, the geometric information of individual point is replaced by the geometry of the voxel. And the problem of uneven point density can be solved, and during the estimation of the geometric information, the use of model-fitting or other approximation methods can suppress outliers and noise. In Zolanvari and Laefer (2016), the slices of the point cloud is utilized as basic unit to extract the boundary of windows and facades, showing a good efficiency with low computational costs. However, for these kinds of methods, the granularity of the basic unit is influential (Vo et al. 2015). In some cases the subdivided voxel may contain intersecting surfaces or edges. Such non-flat surfaces inside the voxel may cause biases when estimating the geometry of a voxel and additional subdivision is normally needed. Furthermore, for assessing the connection of two points or elements, the majority of the current segmentation methods mainly depend on one or two individual criteria like normal vector consistency (Chen et al. 2014), points density (Aljumaily, Laefer, and Cuadra 2017), or surface relations (Stein et al. 2014). However, using single geometric cue seems not reliable, and integrating multiple geometric cues may be a better solution.

Based on voxel-based data structure, we propose a novel robust region-growing clustering methodology for segmenting rooftops from ALS dataset. Our contributions are as follows: (1) Segment clustering algorithm: a voxel-based clustering algorithm based on the smoothness, continuity, and convexity is proposed to dynamically cluster adjacent voxels into segments. (2) Rooftop classification method: an object-based spectral clustering approach is proposed to efficiently and effectively distinguish the roofs.

2. Methodology

Our method consists of following five steps: voxelization, estimation of voxel attribute, calculation of geometric cues, region growing of voxels, and selection of roofs. The processing workflow is sketched in Figure 1, with key steps and sample results illustrated.

2.1. *Voxelization*

The point cloud is rasterized by a 3D cubic grid with an octree structure. The aim of utilizing the octree-based voxel structure in our work is threefold (Vo et al. 2015): (1) Organizing points (i.e.,
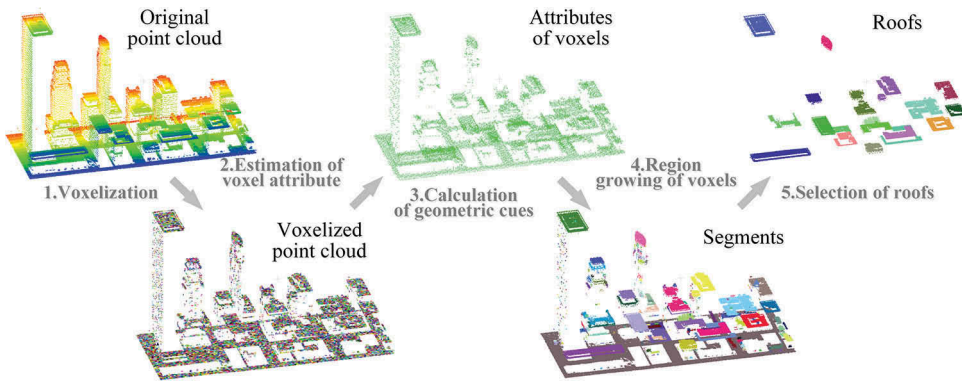
Figure 1. Workflow of the proposed roof segmentation approach.

indexing the unorganized point cloud); (2) Constructing the rasterized representation of points (i.e., simplifying the dataset and suppressing the outliers and noise); (3) Defining neighboring relations of generated voxels as well as the points within them. The points located in the same cubic is clustered as a voxel. The relations between voxels are directly obtained from the octree. Selecting the size of voxels is a trade-off between the efficiency and the preservation of details. Here, the voxel size is determined according to the demands of application empirically.

2.2. Segments generation

2.2.1. Estimation of voxel attribute

The attribute of each voxel is the unary feature of each voxel delineating the geometric attributes of points within it. To represent the points with in each voxel, the common implicit plane (Dutta, Engels, and Hahn 2014) is firstly utilized:

$$\mathbf{N} \cdot \mathbf{X} - X^{\mathrm{d}} = 0 \tag{1}$$

where $\mathbf{N}$ stands for the normal vector of the approximate plane and $\mathbf{X}$ denotes the centroid of points within the voxel V. While X^{d} is the distance from the plane to the origin O (see Figure 2(a)). By the use of the approximate plane, the attribute of a voxel can be expressed by $\mathbf{X}$, $\mathbf{N}$, and X^{d}. $\mathbf{N}$ is obtained from the eigen vectors of points coordinates via PCA of the covariance matrix. However, considering noise and outliers always existing in point clouds, the conventional PCA of the covariance matrix is error-prone. The RPCA strategy is adopted in lieu of conventional PCA method to calculate more accurate $\mathbf{N}$ and centroid $\mathbf{X}$ by yielding outlier free dataset, the points of which is selected by Maximum Consistency with Minimum Distance (MCMD) algorithm (Nurunnabi, West, and Belton 2015) measuring the Mahalanobis Distance (MD). The selection of inliers of points within the voxel consists of three major steps:

- Fitting of the approximate plane: An approximate plane is festimated by the conventional PCA method, with the centroid $\mathbf{p}_c$ and the inverse of covariance matrix $\mathbf{M}^{-1}$ obtained.
- Measuring of MD: The MD of $\mathbf{p}_i$ is calculated using the following equation,where k is the number of points within the voxel, and T means transpose:
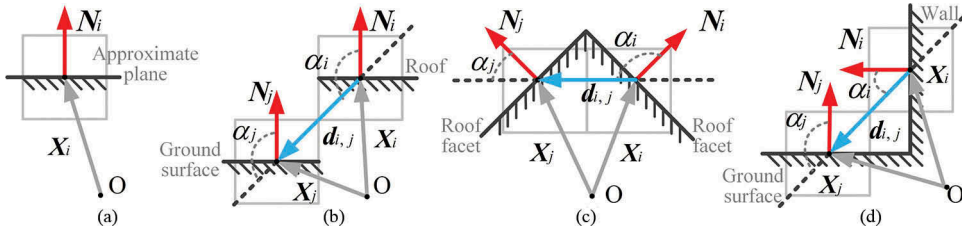
Figure 2. (a) The approximate plane. (b)"stair-like" (c) convex, and (d) concave connections.

$$\mathrm{MD}_i = \sqrt{(\mathbf{p}_i - \mathbf{p}_c)^\mathsf{T} M^{-1}(\mathbf{p}_i - \mathbf{p}_c)}, i = 1, 2, \cdots, k \tag{2}$$

- Selection of inliers: Points having the MD smaller than $\sqrt{\mathcal{X}^2_{m,0.975}} = 3.075$ Nurunnabi, West, and Belton 2015) is selected as the inliers for the RPCA, as the MD following a Chi-square distribution with a degree of freedom m. Namely, only those points with the probability of being inliers larger than 0.975 is selected.

The eigenvector corresponding to the smallest eigenvalue of the covariance matrix from the outlier free dataset is determined as the obtained robust principal component, which is used to estimate the robust **N** and **X**.

2.2.2. Calculation of geometric cues

Geometric cues are binary features characterising the geometric relation between two adjacent voxels, namely the way that two adjacent approximate planes are connected, which are used to estimate the regrowing criteria. In Figure 2, three assumed connection types of approximate planes of voxels are illustrated: 'stair-like', convex, and concave. The 'stair-like' is designed to represent the connection between roofs and parallel ground surfaces with parallel positions but different heights, which should be disconnected during the segmentation. The continuity represents teh ideal connections between adjacent facets belonging to the same roof of a building. The concave connection relates to the case of connected vertical walls and horizontal surface, which should also be disconnected. The convex one is mimicking the ridges of adjacent facet for a building roof (e.g., the hipped, gable, or pinnacle roofs) determined as connected surfaces, so that the entire roof is segmented simultaneously. Based on these assumptions and the attribute of voxel, geometric cues are defined by the use of smoothness (Awrangjeb and Fraser 2014), continuity, and convexity criterion (Stein et al. 2014). The smoothness D^s is defined by the angle difference of normal vectors $\mathbf{N}_i$ and $\mathbf{N}_j$: $D^s_{i,j} = \mathbf{N}_i \cdot \mathbf{N}_j$. The continuity D^d considers the 'stair-like' surfaces (see Figure 2(b)), which is defined by $D^d_{i,j} = (X^d_i - X^s_{i,j})^2 + (X^d_j - X^s_{j,i})^2$, where $X^s_{i,j} = \mathbf{N}_i \cdot \mathbf{X}_j$, $X^s_{j,i} = \mathbf{N}_j \cdot \mathbf{X}_i$, $\mathbf{X}_i$ and $\mathbf{X}_j$ are centroids of V_i and V_j, and X^d_i and X^d_j are the distances from O to the centroids of V_i and V_j respectively. The convexity criterion D^c denotes the 3D convex (see Figure 2(c)) or concave (see Figure 2(c)) relationship connecting surfaces formed by approximate planes of two adjacent voxels V_i and V_j, inferred from the relation of $\mathbf{N}_i$ and $\mathbf{N}_j$ and the vector $\mathbf{d}_{i,j}$ joining their centroids $\mathbf{X}_i$ and $\mathbf{X}_j$. As shown in Figure 2(b-d), the angles a_i and a_j are calculated, where $\mathbf{d}_{i,j} = (\mathbf{X}_i - \mathbf{X}_j)/||\mathbf{X}_i - \mathbf{X}_j||$. If $a_i - a_j > \theta$, the surface connection type is defined as a convex connection, where θ is the threshold for determining convexity. Otherwise, it is considered as a concave connection. θ is

calculated by a sigmoid function determined by the difference of a_i and a_j, following the statement in (Stein et al. 2014). Convex connections are preserved while concave connections should be disconnected based on the degree of convexity criterion D^c:

$$D_{i,j}^c = \begin{cases} (a_i - a_j)^2 & \text{if } a_i - a_j > \theta \\ 2 & \text{else} \end{cases} \tag{3}$$

Considering these three factors, $G_{i,j}$, the connectivity of two voxels V_i and V_j, is calculated according to Eq. 4:

$$G_{i,j} = \prod_k (1 - \exp(-\frac{(D_{i,j}^k)^2}{2\lambda_k^2})) \tag{4}$$

where λ_k denote the bandwidth of the Gaussian kernel and $k \in [s, d, c]$, adjusting the importance of smoothness, continuity, and convexity, respectively, which are set to 0.1.

2.2.3. *Merging voxels*

Once the geometric cues between all the voxels pairs are obtained, the connection between adjacent voxels is finally determined by using a given threshold $\gamma \in [0, 1]$. If $G_{i,j} > \gamma$, this voxel pair are connected. Otherwise, it is disconnected. For initial clustering voxels used as growing seeds, the ones having a change of curvature $C_e = e_1/(e_1 + e_2 + e_3)$ with $C_e \in [0, 1)$ (Weinmann et al. 2015) smaller than the given threshold β will be selected as seeds. Here, the eigenvalues e_1, e_2, e_3 used for calculating C_e is calculated from RPCA of the covariance matrix from inliers obtained in Section 2.2.1. The growing process will merge all the connected voxels as a complete segment.

2.3. *Selection of roofs*

For the obtained segments, a object-based spectral clustering is carried out to distinguish the segments belonging to roofs, with all the segments grouped into two classes: the roof surface and other objects. Here, an assumption is made that the segments of roofs consisting of merely planar surfaces have distinctiveness in geometry (e.g., normal vector, height, shapes) than other objects in the scene. The attribute of a segment is described by linearity S_l, planarity S_p, scattering S_s, omnivariance S_o, anisotropy S_a, eigenentropy S_e, sum of eigenvalues S_m, and change of curvature S_c (Weinmann et al. 2015). A feature histogram H with bins encoding these attributes is generated for each segment. The difference ΔH of two histograms is measured by the use of histogram intersection kernel (Stein et al. 2014). Then, an unsupervised binary classification using the spectral clustering (Von Luxburg 2007; Alexandrov 2014) is conducted. As required by the spectral clustering, a adjacency matrix of the indirect graph G delineating the similarity between the feature histograms of two segments is constructed. The weight $W_{i,j}$ of the adjacency matrix G is calculated as follows:

$$W_{i,j} = \exp(\frac{-||\Delta H||_2}{2\sigma^2}) \tag{5}$$

where σ is the scale factor of the Gaussian kernel related to the sensitivity of the weight. Then, eigenvectors of the Laplacian matrix L is calculated via EVD and diagonal matrix of G. A k-means clustering is done for the eigenvectors corresponding to two smallest eigenvalues,

in order to label the final classes. The ground surface is removed by analyzing peaks in the projecting histogram described in (Oesau, Lafarge, and Alliez 2014). Small and fractional segments (less than 50 points) are removed before selection.

3. Experimental results and discussion

3.1. *Datasets and evaluation metrics*

Experiments are performed on three ALS datasets provided by ISPRS benchmark tests (Cramer 2010) and University College Dublin (Aljumaily, Laefer, and Cuadra 2017). The Vaihingen (VH) dataset was obtained over Vaihingen, Germany, by the use of a Leica ALS50, with the point density of around 4 points/m^2. Whereas the Toronto (TR) dataset was acquired in the downtown area of Toronto, Canada, using Optechs airborne laser scanner with a density of around 6 points/m^2. The Dublin (DB) dataset is of high quality having a much higher point density of around 225 points/m^2, which is introduced to see the situation of dealing with a higher density dataset. Three study areas are selected with varying point density and different rooftop structures (see Figure 3).

Two representative methods, including the point-based region growing (PRG) (Rabbani, Van Den Heuvel, and Vosselmann 2006) which is the classical region growing method, and the popular Locally Convex Connected Patches (LCCP) (Stein et al. 2014) utilizing the voxel structure, are used as reference methods and implemented by the use of Point Cloud Library (PCL) (Rusu and Cousins 2011). Different conditions of our VRG method using conventional PCA and RPCA are compared, for investigating the effectiveness of RPCA. Two subareas (see Figure 3(a,b)) are manually segmented from the study areas as ground truth dataset, with roofs rendered with red colour. The quantitative evaluation compares segments against ground truth using the metheod described in Awrangjeb and Fraser (2014); Vo et al. (2015). Three standard metrics, Completeness(Comp), Correctness (Corr), and Quality (Qual), are adopted to assess the quality of segmentation results. Note that unlike the one-to-one correspondence used in (Rutzinger, Rottensteiner, and Pfeifer 2009), the strategy proposed in (Xu et al. 2015) is adopted when finding the correspondence between the reference and the segments. Specifically, for one segment, if it corresponds to two reference segments (i.e., one-to-many), both of these two ground truth segments are taken into consideration when calculating the true positive rate. Besides, parameters and thresholds used are listed in Table 1, including the size of neighborhood (SN) for PRG, voxel size (VS) and supervoxel size (SVS) for VRG and LCCP, thresholds for normal angle difference (TD) for all methods, growing threshold γ for VRG, and so on. The voxel size or neighborhood is the most significant one, namely the granularity of the entire voxel structure. In theory, the larger the voxel is, the more details of the scene will be blurred. For VH and TR datasets with low point density, a large size
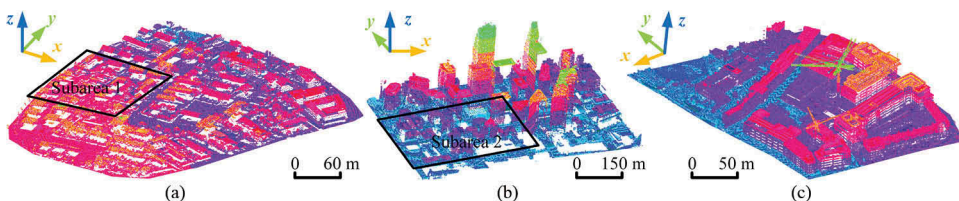

Figure 3. Point clouds rendered by heights with varying colours. The lighter the colour of a point, the higher the rendered point is. (a) Vanhingen, (b) Toronto, and (c) Dublin.

Table 1. Parameters used in methods.

Method	Dataset		
	VH	TR	DB
PRG	SN = 1.5m; TD = 15°;	SN = 3.0m; TD = 15°	Not used
LCCP	VS = 1.5m; SVS = 3.0m; TD = 15°;	VS = 3.0m; SVS = 6.0m; TD = 15°	Not used
VRG	SV = 1.5m; SN = 3.0m; TD = 15°; γ=0.1; σ=0.3; λ_k=0.1	SV = 3.0m; SN = 6.0m; TD = 15°; γ=0.1; σ=0.3; λ_k=0.1	SV = 0.75m; SN = 1.5m; TD = 15°; γ=0.1; σ=0.3; λ_k=0.1

of voxel and neighborhood is selected, while for the dense DB dataset, a smaller voxel is applied. Parameters are determined empirically. For voxel-based methods (i.e., VRG and LCCP), the voxel resolution of them is equal to the size of the neighborhood used in the point-based method (i.e., PRG) when using same dataset. Our experiments hope the normal vectors used in different methods can be calculated in the same situation: all normal vectors are estimated by points in the neighborhoods of the similar size. The supervoxel size and the neighborhood of VRG is twice as large as the voxel size, corresponding to the adjacencies of the center one.

3.2. Segmentation results

In Figure 4, qualitative segmentation outputs of study areas using our proposed method are illustrated. The majority of the roofs are segmented in all the three study areas, with clear edges. However, over- and under-segmentations also occur for some roofs in the VH dataset, especially for the roofs covered by the tree crowns. One possible reason is due to the occlusion caused by tree crowns, resulting in the discontinuity and missing points of objects. For small objects, the size of voxel will also affect the quality of segmentation. Besides, for the result of DB dataset, there are also obvious under-segmentations. This is because the scene of DB dataset covers the area with many crowded buildings, and for two adjacent buildings joined together, our approach may regard them as a single building. As a common problem for building extraction, this phenomenon has reported and discussed in (Aljumaily, Laefer, and Cuadra 2017), and in their work, a density based clustering method is applied to the dense DB dataset, with impressive good results achieved. This may be a possible solution for the high density datasets like DB. The quantitative evaluation results using datasets of subareas are listed in Table 2. It is evident that our VRG methods outperform the other methods for these two testing datasets, no matter whether the RPCA is applied or not. The Qual values are better than 0.6. By adopting RPCA instead of the conventional PCA, the quality of segments is further improved, in particular for the dataset of Vaihingen. This is because the datasets of Vaihingen includes more outliers and occlusions, so that RPCA can significantly enhance the segmentation performance. Moreover, considering the execution time of using different methods, it is easily found that our VRG methods are much efficient than the traditional point-based one, but inferior to the LCCP using supervoxels to reduce computation cost and be conductive to the boundary keeping.

In Figure. 5(a-c), selected roofs are illustrated. In study areas, there are in total 44, 101, and 74 roof surfaces selected, respectively. To assess the correctness of the selection results, the roof selection results using datasets of two subareas are shown in Figure 5(d), with evaluation results given in Table 3. The majority of the selected roofs are correct ones, especially for the results of TR dataset, only 3 and 4 selected roofs are the type I and II error. However, for the result of using Vaihingen dataset, more errors occur, which are largely resulted from the inferior segmentation quality. For example, the under-segmented surfaces will directly lead to
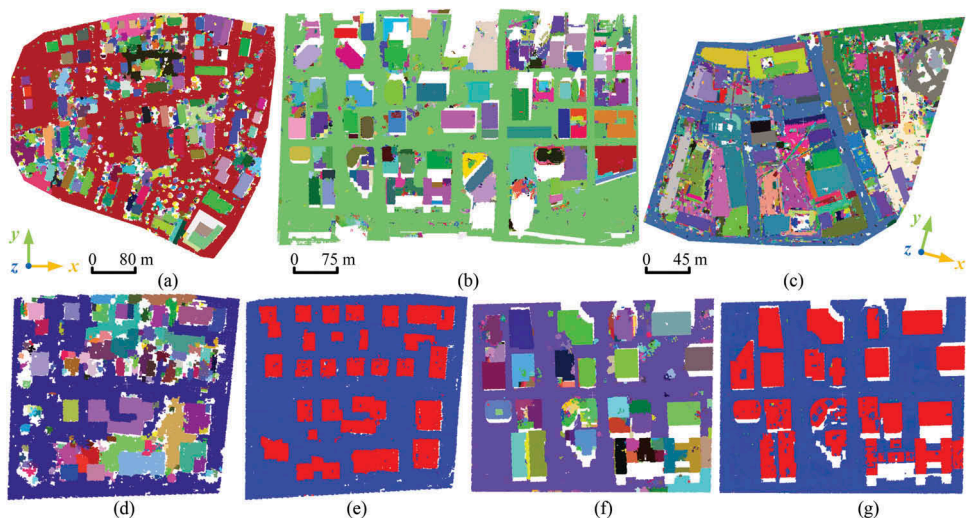
Figure 4. Segmented results of study areas (a) Dublin, (b)Vaihingen, and (c)Toronto. Segmentation results of subareas and corresponding ground truth (d) Vaihingen and (e) Toronto. For illustration, the segments are rendered with different colours randomly. In the ground truth, the building roofs are rendered with red colour.

Table 2. Evaluation of segmentation results using datasets of subareas.

Method	Vaihingen: 70,000 points				Toronto: 300,000 points			
	Comp	Corr	Qual	Time (ms)	Comp	Corr	Qual	Time (ms)
PRG	0.6865	0.7465	0.5567	3.58	0.5931	0.8885	0.5520	16.57
LCCP	0.6323	0.7308	0.5128	1.51	0.6298	0.7081	0.5001	4.73
VRG+PCA	0.8145	0.7527	0.6426	2.57	0.8964	0.6445	0.5998	8.09
VRG+RPCA	0.8667	0.7941	0.7077	2.83	0.7648	0.7535	0.6117	8.34

the type II errors in the roof selection process. Note that the segmentation and selection results using the whole scene of dataset and its corresponding subareas are slightly different. The reason is due to the subdivision of the octree, during which different sizes of point clouds are organized with different initial bounding boxes. For example, edges of the same object are organized into different voxels, when datasets are of various size resulting in different sizes of bounding boxes used for subdivision. The selection of the optimal voxel size will be further investigated. Besides, large-scale datasets are not considered. For large-scale datasets, the adaptivity is normally required, which should be further improved.

4. Conclusion

In this work, a novel point cloud segmentation method termed VRG is contributed, combining the merits of voxel structure and RPCA, which is designed to automatically and adaptively partition ALS point cloud for extracting building roofs. Our methods are tested in different scenes using point clouds generated from ALS, and compared its results with those of representative reference methods. The qualitative and quantitative results reveal that our method outperform some representative algorithms in segmentation using our testing datasets under a complex situation, especially for datasets of a low point density, with overall Quality measure better than 0.7 and 0.6.
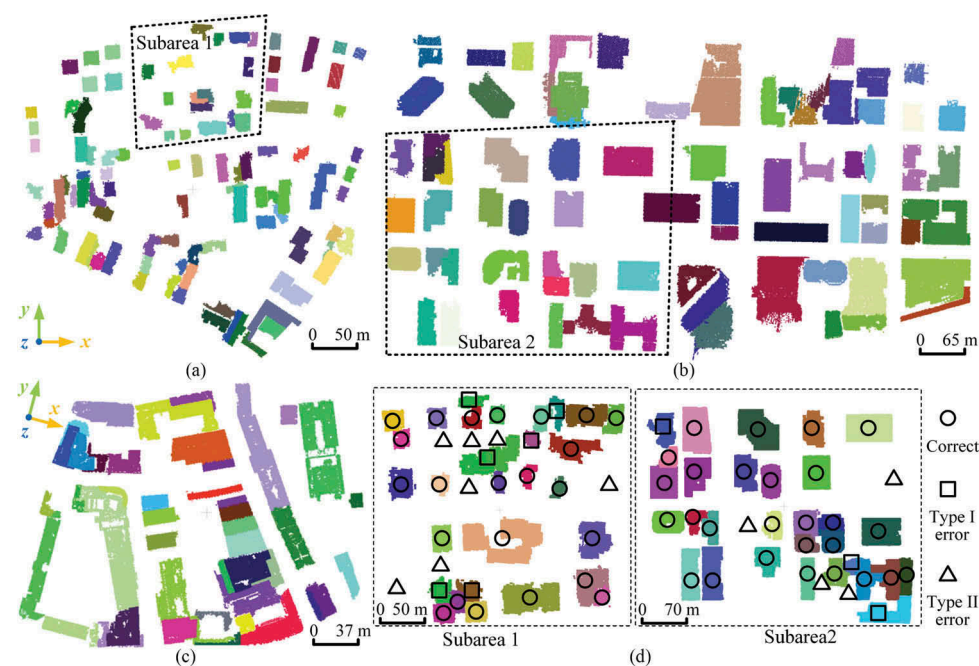
Figure 5. Selected roofs of study areas (a) Vaihingen, (b)Toronto, and (c) Dublin. (d) Evaluation using subareas, with results marked. The segments are rendered with different colours randomly.

Table 3. Summary accuracy of roof segmentation.

Dataset	Number correct	Number of type I error roofs	Number of type II error roofs
Vaihingen	22	6	7
Toronto	27	3	4

ORCID

Yusheng Xu 🅳 http://orcid.org/0000-0001-5571-7808

References

Alexandrov, S. 2014. *Geometrical Segmentation of Point Cloud Data by Spectral Analysis*. Sankt Augustin Germany: Hochschule Bonn-Rhein-Sieg.

Aljumaily, H., D. F. Laefer, and D. Cuadra. 2015. "Big-Data Approach for Three-Dimensional Building Extraction from Aerial Laser Scanning." *Journal of Computing in Civil Engineering* 30 (3): 04015049. doi:10.1061/(ASCE)CP.1943-5487.0000524.

Aljumaily, H., D. F. Laefer, and D. Cuadra. 2017. "Urban Point Cloud Mining Based on Density Clustering and Mapreduce." *Journal of Computing in Civil Engineering* 31: 04017021. doi:10.1061/(ASCE)CP.1943-5487.0000674.

Awrangjeb, M., and C. S. Fraser. 2014. "Automatic Segmentation of Raw Lidar Data for Extraction of Building Roofs." *Remote Sensing* 6 (5): 3716–3751. doi:10.3390/rs6053716.

Chen, D., L. Zhang, J. Li, and R. Liu. 2012. "Urban Building Roof Segmentation from Airborne Lidar Point Clouds." *International Journal of Remote Sensing* 33 (20): 6497–6515. doi:10.1080/01431161.2012.690083.

Chen, D., L. Zhang, P. T. Mathiopoulos, and X. Huang. 2014. "A Methodology for Automated Segmentation and Reconstruction of Urban 3-D Buildings from Als Point Clouds." *IEEE Journal*

of Selected Topics in Applied Earth Observations and Remote Sensing 7 (10): 4199–4217. doi:10.1109/JSTARS.2014.2349003.

Cramer, M. 2010. "The Dgpf-Test on Digital Airborne Camera Evaluation–Overview and Test Design." *Photogrammetrie-Fernerkundung-Geoinformation* 2010 (2): 73–82. doi:10.1127/1432-8364/2010/0041.

Dutta, A., J. Engels, and M. Hahn. 2014. "A Distance-Weighted Graph-Cut Method for the Segmentation of Laser Point Clouds." *ISPRS - International Archives of the Photogrammetry, Remote Sensing and Spatial Information Sciences* XL-3: 81–88. doi:10.5194/isprsarchives-XL-3-81-2014.

Nurunnabi, A., G. West, and D. Belton. 2015. "Outlier Detection and Robust Normal-Curvature Estimation in Mobile Laser Scanning 3d Point Cloud Data." *Pattern Recognition* 48 (4): 1404–1419. doi:10.1016/j.patcog.2014.10.014.

Oesau, S., F. Lafarge, and P. Alliez. 2014. "Indoor Scene Reconstruction Using Feature Sensitive Primitive Extraction and Graph-Cut." *ISPRS Journal of Photogrammetry and Remote Sensing* 90: 68–82. doi:10.1016/j.isprsjprs.2014.02.004.

Rabbani, T., F. Van Den Heuvel, and G. Vosselmann. 2006. "Segmentation of Point Clouds Using Smoothness Constraint." *International Archives Photogramm Remote Sens Spatial Information Sciences* 36 (5): 248–253.

Rusu, R. B., and S. Cousins. 2011. "3d Is Here: Point Cloud Library (PCL)." In *Robotics and Automation (ICRA), 2011 IEEE International Conference On*, edited by A. Bicchi, Shanghai, 1–4. IEEE. doi:10.1109/ICRA.2011.5980567

Rutzinger, M., F. Rottensteiner, and N. Pfeifer. 2009. "A Comparison of Evaluation Techniques for Building Extraction from Airborne Laser Scanning." *IEEE Journal of Selected Topics in Applied Earth Observations and Remote Sensing* 2 (1): 11–20. doi:10.1109/JSTARS.2009.2012488.

Schnabel, R., R. Wahl, and R. Klein. 2007. "Efficient Ransac for Point-Cloud Shape Detection." In *Computer Graphics Forum*. Vol. 26, edited by D. Duke and R. Scopigno, 214–226. Oxford, UK: Blackwell Publishing.

Stein, S., M. Schoeler, J. Papon, and F. Worgotter. 2014. "Object Partitioning Using Local Convexity." In *Proceedings of the IEEE Conference on Computer Vision and Pattern Recognition*, Columbus, OH, 304–311. Conference Publishing Services (CPS). doi:10.1109/CVPR.2014.46

Truong-Hong, L., D. F. Laefer, T. Hinks, and H. Carr. 2013. "Combining an Angle Criterion with Voxelization and the Flying Voxel Method in Reconstructing Building Models from Lidar Data." *Computer-Aided Civil and Infrastructure Engineering* 28 (2): 112–129. doi:10.1111/mice.2013.28.issue-2.

Vo, A.-V., L. Truong-Hong, D. Laefer, D. Tiede, S. Dâ€™, A. Oleire Oltmanns, M. Baraldi, S. G. Moser, and D. Tuia. 2016. "Processing of Extremely High Resolution Lidar and Rgb Data: Outcome of the 2015 Ieee Grss Data Fusion Contestâ€"Part B: 3-D Contest." *IEEE Journal of Selected Topics in Applied Earth Observations and Remote Sensing* 9 (12): 5560–5575. doi:10.1109/JSTARS.2016.2581843.

Vo, A.-V., L. Truong-Hong, D. F. Laefer, and M. Bertolotto. 2015. "Octree-Based Region Growing for Point Cloud Segmentation." *ISPRS Journal of Photogrammetry and Remote Sensing* 104: 88–100. doi:10.1016/j.isprsjprs.2015.01.011.

Von Luxburg, U. 2007. "A Tutorial on Spectral Clustering." *Statistics and Computing* 17 (4): 395–416. doi:10.1007/s11222-007-9033-z.

Wang, H., W. Zhang, Y. Chen, M. Chen, and K. Yan. 2015. "Semantic Decomposition and Reconstruction of Compound Buildings with Symmetric Roofs from Lidar Data and Aerial Imagery." *Remote Sensing* 7 (10): 13945–13974. doi:10.3390/rs71013945.

Weinmann, M., B. Jutzi, S. Hinz, and C. Mallet. 2015. "Semantic Point Cloud Interpretation Based on Optimal Neighborhoods, Relevant Features and Efficient Classifiers." *ISPRS Journal of Photogrammetry and Remote Sensing* 105: 286–304. doi:10.1016/j.isprsjprs.2015.01.016.

Xu, B., W. Jiang, J. Shan, J. Zhang, and L. Li. 2015. "Investigation on the Weighted Ransac Approaches for Building Roof Plane Segmentation from Lidar Point Clouds." *Remote Sensing* 8 (1): 5. doi:10.3390/rs8010005.

Zolanvari, S. I., and D. F. Laefer. 2016. "Slicing Method for Curved Façade and Window Extraction from Point Clouds." *ISPRS Journal of Photogrammetry and Remote Sensing* 119: 334–346. doi:10.1016/j.isprsjprs.2016.06.011.